Mapping the Ligand-Binding Site on a G Protein-Coupled Receptor (GPCR) Using Genetically Encoded Photocrosslinkers

ARTICLE *in* BIOCHEMISTRY · MARCH 2011

Impact Factor: 3.02 · DOI: 10.1021/bi200214r · Source: PubMed

4 AUTHORS, INCLUDING:

Thomas Huber
The Rockefeller University
72 PUBLICATIONS **1,541** CITATIONS
SEE PROFILE

Pallavi Sachdev
Eisai Japan
79 PUBLICATIONS **1,356** CITATIONS
SEE PROFILE

Thomas Sakmar
The Rockefeller University
218 PUBLICATIONS **10,815** CITATIONS
SEE PROFILE

Published in final edited form as:
Biochemistry. 2011 May 3; 50(17): 3411–3413. doi:10.1021/bi200214r.

Mapping the Ligand-binding Site on a GPCR Using Genetically-encoded Photocrosslinkers

Amy Grunbeck, **Thomas Huber**, **Pallavi Sachdev**, and **Thomas P. Sakmar***
Laboratory of Molecular Biology and Biochemistry, The Rockefeller University, New York, NY

Abstract

We developed a general cell-based photocrosslinking approach to investigate the binding interfaces necessary for the formation of G protein-coupled receptor (GPCR) signaling complexes. The two photoactivatable unnatural amino acids *p*-benzoyl-L-phenylalanine and *p*-azido-L-phenylalanine were incorporated by amber codon suppression technology into CXC chemokine receptor 4 (CXCR4). We then probed the ligand-binding site for the HIV-1 co-receptor blocker, T140, using a fluorescein-labeled T140 analogue. Among eight amino acid positions tested, we found a unique UV-light dependent crosslink specifically between residue 189 and T140. These results are evaluated with molecular modeling using the crystal structure of CXCR4 bound to CVX15.

GPCRs are dynamic membrane proteins that trigger and regulate cellular signaling pathways. In the classical paradigm of GPCR signaling, an extracellular ligand binds to a specific receptor to activate a heterotrimeric G protein. GPCRs also activate beta-arrestin-dependent kinase pathways (1). To facilitate GPCR-targeted drug development, it is important to understand how ligands bind to and modulate GPCR structure and function. However, common techniques for examining the structural aspects of receptor-ligand complexes that rely on reconstitution, including crystallography and biophysical methods, are limited by the inherent instability of receptors in solution and the requirement for a membrane environment. Our aim is to develop a method to study low abundance and/or transient receptor complexes in the native cellular membrane environment.

One approach to gain information about GPCR structure and function is to trap a receptor-ligand complex using photoactivatable cross-linkers. Although a number of successful receptor-ligand crosslinking experiments have been reported, the general strategy of synthesizing ligands with photoactivatable groups is conceptually limited and technically challenging (2, 3). Even if crosslinking can be achieved, identifying the site of the crosslink is difficult, and sometimes not possible. We have adapted the amber stop codon suppression technology to incorporate site-specifically two unnatural amino acid (UAA) photocrosslinkers, p-benzoyl-L-phenylalanine (BzF) and p-azido-L-phenylalanine (azF), into GPCRs heterologously expressed in mammalian cells (4). This approach provides a means to capture a covalent GPCR-ligand complex and to map the specific sites in the receptor that are capable of reacting with any particular binding partner of interest. In addition to investigating known GPCR complexes, this site-directed photocrosslinking technology can be applied in principle to identify the native ligands for orphan GPCRs and other novel GPCR modulators. Here, we show how this methodology can be used in cells to probe the binding interface between CXCR4 and T140, a CXCR4-specific inhibitor.

*To whom correspondence should be addressed. sakmar@rockefeller.edu. Phone: (212) 327-8288. Fax: (212) 327-7904.

SUPPORTING INFORMATION AVAILABLE
Detailed experimental methods and supplementary figures can be accessed free of charge online at http://pubs.acs.org.

CXCR4 is a chemokine receptor that mediates directed cell migration in development and during inflammation and cancer metastasis. It is also known to be a co-receptor for cellular HIV-1 entry (5). The discovery that CXCL12, the chemokine ligand for CXCR4, blocks virus entry into host cells identified CXCR4 as a potential target for HIV-1 entry inhibitors (6). The small molecule CXCR4 antagonist, AMD3100, was the first proof-of-concept HIV-1 entry blocker (7), which led to the development of CCR5-targeted entry blockers (8). CXCR4 inhibitors also induce the mobilization of hematopoietic stem cells by disrupting the interaction between CXCR4 and CXCL12, which is necessary for retaining HSCs in the bone marrow (9–11). For these reasons CXCR4 is an important therapeutic target for cancer and HIV treatment.

T140, a 14-residue cyclic peptide CXCR4 antagonist, blocks HIV-1 entry (12). We used the CXCR4-T140 complex to validate a site-specific crosslinking technology for identifying GPCR-ligand binding interfaces. Earlier CXCR4-T140 complex models were developed using mutagenesis and crosslinking techniques, which included chemical- and photocrosslinking using a T140 analogue containing BzF. These strategies required digestion of CXCR4 to determine the site in the receptor that was covalently bound to the T140 analogue (13, 14). These experiments were only able to resolve a peptide fragment of CXCR4 that was bound to T140. CXCR4-T140 complex models derived from these studies differ from the crystal structure of CXCR4 bound to CVX15, a 16-residue peptide with high homology to T140 (15). The difference between the CXCR4-T140 complex models and the crystal structure of the CXCR4-CVX15 complex result from the inability of earlier crosslinking techniques to identify the exact site in CXCR4 that crosslinked with T140. We aimed to develop a site-directed photocrosslinking technology to predict more accurate models of GPCR-ligand complexes even in the absence of available crystal structures.

The site-directed crosslinking technology relies on a specific and sensitive detection method to identify both binding partners in the crosslinked complex. We accomplish this by attaching a unique antibody reactive tag on each complex component. CXCR4 contains a C-terminal C9 epitope tag for mAb 1D4, and T140 is labeled with fluorescein (Fig. 1a). The fluorescein tag is used for specific detection by immunoblot analysis using an anti-fluorescein antibody. Fluorescein was directly conjugated to Lys 8 on T140, which does not interfere with binding to CXCR4 (16, 17). Thus, fluorescein-T140 (FL-T140) is a suitable ligand to validate the application of the site-directed crosslinking technology.

First, to optimize conditions for crosslinking and detection of the FL-T140/CXCR4 complex, we used a T140 analogue containing fluorescein and BzF at position 10 (FL-T140-BzF). This T140 derivative has been reported to crosslink to CXCR4 and serves as a positive control (18). We also demonstrated that FL-T140-BzF crosslinks specifically to CXCR4 in cell culture. CXCR4-transfected HEK293T cells were incubated with FL-T140-BzF prior to UV light exposure. Following UV exposure, the cells were solubilized in detergent and CXCR4 was immunopurified from the lysate using sepharose beads conjugated to the 1D4 mAb. An immunoblot of the purified samples showed a UV-treatment-dependent band on the anti-fluorescein blot at the molecular mass of the receptor (Fig. S1 of the Supporting Information). This indicates the existence of a covalent complex between FL-T140-BzF and CXCR4, which was not detected if a 100-fold excess of unlabeled T140 was present. Additionally, no crosslink was detected in untransfected cells or to CCR5, another chemokine receptor with high homology to CXCR4, demonstrating the specificity of T140 for CXCR4. The fluorescein moiety also proved to be a specific and sensitive detection tag on an immunoblot using an anti-fluorescein polyclonal antibody.

For the site-specific crosslinking experiments from the side of the receptor, residues in CXCR4 were chosen for replacement with a photocrosslinking UAA based on previously

reported biochemical and molecular modeling data. The CXCR4 schematic shows the sites, which when mutated to an Ala, caused a decrease in T140 inhibition of HIV-1 entry (Fig. 1b) (13). Although in principle any amino acid residue can be targeted for amber codon suppression, we chose Phe residues in close proximity to these sites for replacement with BzF or azF in order to make mutations that would be the least likely to perturb the native structure of the receptor. These UAAs were incorporated one-by-one at each position using an engineered BzF or azF amino-acyl tRNA synthetase and suppressor tRNA pair that recognize an amber stop codon (UAG) on the receptor mRNA (4). Incorporation of BzF at the position of the amber stop codon in CXCR4 was confirmed by immunoblot to detect full-length receptor (Fig. S2 of the Supporting Information).

Introducing UAAs into GPCRs alters the native sequence of the receptor, but the proper folding and function of the receptor can be retained, as has been reported for the incorporation of UAAs into other GPCRs, including rhodopsin and CCR5 (4, 19, 20). For this experiment, we determined whether incorporation of BzF into CXCR4 affects binding to T140 by examining the crosslinking efficiency of FL-T140-BzF to each of the CXCR4 BzF containing mutants. All of the mutants crosslinked to FL-T140-BzF, indicating that T140 is able to bind to the CXCR4 variants containing BzF (Fig. S3 of the Supporting Information). Each of the CXCR4 BzF mutants were then tested for UV-induced crosslinking to FL-T140. HEK293T cells expressing the CXCR4 BzF mutants were incubated with FL-T140 and then exposed to UV light. The cells were then scraped and solubilized in detergent and the lysate was separated on a SDS-PAGE gel and subjected to immunoblot analysis.

The results from this series of experiments showed an anti-fluorescein positive band at the molecular mass of CXCR4 only when BzF was introduced at position 189 (Fig. 1c and Fig. S4 of the Supporting Information) or when BzF was at position 10 in FL-T140-BzF (Fig. 1d). These results suggest that Phe 189 is within close proximity to the T140 binding site, whereas the other residues in CXCR4 examined are not. The same crosslinking experiment was also performed in the presence of 100-fold excess of unlabeled T140. In this case no band was detected with the anti-fluorescein antibody, which demonstrates the specificity of the crosslink at position 189 for T140 (Fig. 1e). The same results were also seen with azF at the same sites in CXCR4 (Fig. S5 of the Supporting Information), although background crosslinking without UV treatment was significantly higher when using azF as compared to BzF (Fig. 1f). On the other hand, one advantage of using azF over BzF is that the size of the side chain is significantly smaller and less perturbing to the native structure of the protein.

Evaluating our findings in the context of the crystal structure of CXCR4 bound to CVX15 verifies the application of this technology to identify residues in CXCR4 that are within close proximity to the T140 binding site. Assuming that T140 has a similar binding site as CVX15, Phe189 immediately stands out from the other sites as being within crosslinking distance to the ligand (Fig. 2a, b). Since the crystal structure is limited to a single static image, we also carried out computational modeling to predict the possible orientations of BzF at each of these sites (Fig. 2c). We calculated the distance between the center-of-mass of the reactive carbonyl in BzF to the nearest atom in the CVX15 peptide for each of the possible orientations of BzF at each position. BzF at position 189 was the only site to have a reasonably high probability of being within 2 to 5 Å from the peptide – all other potential carbonyl-CVX15 atom pairs were greater than 5 Å apart (Fig. 2d). This agrees with other reports that the minimum required distance to form a crosslink with a benzophenone group is approximately 3 Å (21, 22).

The main ligand-binding pocket for family A GPCRs is defined as the pocket between the extracellular segments of transmembrane helices III, V, and VI (23). The CXCR4-CVX15

crystal structure shows that Phe189 is within extracellular loop 2 of CXCR4, which borders the main ligand-binding pocket of CXCR4, and lies within a defined distance from bound T140. We plan to use this methodology to map residues in CXCR4 that line the binding site of CXCL12.

In conclusion, we developed a cell-based photocrosslinking method to identify the residues in a GPCR that are within a precise distance from a bound ligand. We have shown that incorporating either BzF or azF results in the same crosslinking sites and that fluorescein serves as a very sensitive and specific epitope tag. This technology should prove useful for investigating the structure of GPCR complexes formed within a live cell. In addition, combining a site-directed photocrosslinking technology with available crystal structures could lead to more accurate models of various conformational states of GPCR signaling complexes, or “signalosomes.”

Supplementary Material

Refer to Web version on PubMed Central for supplementary material.

Acknowledgments

We thank Manija Kazmi and Shixin Ye for helpful discussions and scientific assistance. We also thank Martin Teintze for providing us with FL-T140-BzF and the Proteomic Resource Center at Rockefeller University for the synthesis of the other T140 compounds and Ray Stevens for providing the coordinates for the CXCR4 structure before release. The Tri-Institutional Training Program in Chemical Biology supports A.G. Support was received from NIH ROI EY12049.

References

1. Shenoy SK, Lefkowitz RJ. Sci STKE. 2005; 2005:cm10. [PubMed: 16267056]
2. Nakayama TA, Khorana HG. J Biol Chem. 1990; 265:15762–15769. [PubMed: 2144289]
3. Chen Q, Pinon DI, Miller LJ, Dong MQ. J Biol Chem. 2009; 284:34135–34144. [PubMed: 19815559]
4. Ye SX, Kohrer C, Huber T, Kazmi M, Sachdev P, Yan ECY, Bhagat A, RajBhandary UL, Sakmar TP. J Biol Chem. 2008; 283:1525–1533. [PubMed: 17993461]
5. Feng Y, Broder CC, Kennedy PE, Berger EA. Science. 1996; 272:872–877. [PubMed: 8629022]
6. Oberlin E, Amara A, Bachelerie F, Bessia C, Virelizier JL, ArenzanaSeisdedos F, Schwartz O, Heard JM, ClarkLewis I, Legler DF, Loetscher M, Baggiolini M, Moser B. Nature. 1996; 382:833–835. [PubMed: 8752281]
7. Donzella GA, Schols D, Lin SW, Este JA, Nagashima KA, Maddon PJ, Allaway GP, Sakmar TP, Henson G, De Clercq E, Moore JP. Nat Med. 1998; 4:72–77. [PubMed: 9427609]
8. Seibert C, Sakmar TP. Curr Pharm Des. 2004; 10:2041–2062. [PubMed: 15279544]
9. Hattori K, Heissig B, Tashiro K, Honjo T, Tateno M, Shieh JH, Hackett NR, Quitoriano MS, Crystal RG, Rafii S, Moore MAS. Blood. 2001; 97:3354–3360. [PubMed: 11369624]
10. Liles WC, Broxmeyer HE, Rodger E, Wood B, Hubel K, Cooper S, Hangoc G, Bridger GJ, Henson GW, Calandra G, Dale DC. Blood. 2003; 102:2728–2730. [PubMed: 12855591]
11. Tchernychev B, Ren Y, Sachdev P, Janz JM, Haggis L, O’Shea A, McBride E, Looby R, Deng Q, McMurry T, Kazmi MA, Sakmar TP, Hunt S III, Carlson KE. Proc Natl Acad Sci. 2010; 107:22255–22259. [PubMed: 21139054]
12. Tamamura H, Hori A, Kanzaki N, Hiramatsu K, Mizumoto M, Nakashima H, Yamamoto N, Otaka A, Fujii N. FEBS Lett. 2003; 550:79–83. [PubMed: 12935890]
13. Trent JO, Wang ZX, Murray JL, Shao WH, Tamamura H, Fujii N, Peiper SC. J Biol Chem. 2003; 278:47136–47144. [PubMed: 12958314]
14. Boulais PE, Dulude D, Cabana J, Heveker N, Escher E, Lavigne P, Leduc R. Biochem Pharm. 2009; 78:1382–1390. [PubMed: 19631193]

15. Wu B, Chien EY, Mol CD, Fenalti G, Liu W, Katritch V, Abagyan R, Brooun A, Wells P, Bi FC, Hamel DJ, Kuhn P, Handel TM, Cherezov V, Stevens RC. Science. 2010; 330:1066–1071. [PubMed: 20929726]
16. Oishi S, Masuda R, Evans B, Ueda S, Goto Y, Ohno H, Hirasawa A, Tsujimoto G, Wang ZX, Peiper SC, Naito T, Kodama E, Matsuoka M, Fujii N. ChemBioChem. 2008; 9:1154–1158. [PubMed: 18412193]
17. Nomura W, Tanabe Y, Tsutsumi H, Tanaka T, Ohba K, Yamamoto N, Tamamura H. Bioconjug Chem. 2008; 19:1917–1920. [PubMed: 18707146]
18. Wilkinson RA, Pincus SH, Shepard JB, Walton SK, Bergin EP, Labib M, Teintze M. Antimicrob Agents Chemother. 2011; 55:255–263. [PubMed: 20937786]
19. Ye SX, Huber T, Vogel R, Sakmar TP. Nat Chem Biol. 2009; 5:397–399. [PubMed: 19396177]
20. Ye SX, Zaitseva E, Caltabiano G, Schertler GFX, Sakmar TP, Deupi X, Vogel R. Nature. 2010; 464:1386–1389. [PubMed: 20383122]
21. Dorman G, Prestwich GD. Biochemistry. 1994; 33:5661–5673. [PubMed: 8180191]
22. Sato S, Mimasu S, Sato A, Hino N, Sakamoto K, Umehara T, Yokoyama S. Biochemistry. 2011; 50:250–257.
23. Rosenkilde MM, Benned-Jensen T, Frimurer TM, Schwartz TW. Trends Pharmacol Sci. 2010; 31:567–574. [PubMed: 20870300]
24. Wittelsberger A, Thomas BE, Mierke DF, Rosenblatt M. FEBS Lett. 2006; 580:1872–1876. [PubMed: 16516210]

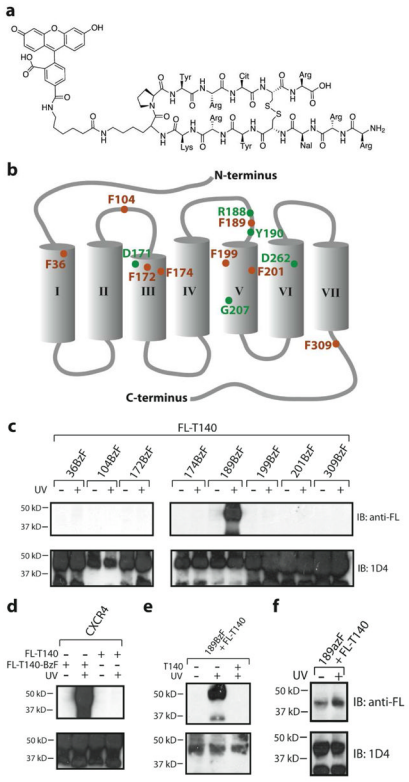

Figure 1.

Photocrosslinking of CXCR4 UAA mutants to FL-T140. (a) Chemical structure of FL-T140. (b) CXCR4 schematic highlighting sites important for T140 binding (green) as determined by alanine scanning (13) and positions where a UAA was incorporated (orange). (c) Western blot analysis of lysate from HEK293T cells expressing CXCR4 BzF mutants that were exposed to UV light in presence of FL-T140. CXCR4 189BzF was the only CXCR4 BzF mutant that crosslinked to FL-T140. (d) As a positive control FL-T140-BzF was crosslinked to WT CXCR4. Background crosslinking was not detected between WT CXCR4 and FL-T140. (e) Crosslinking of CXCR4 189BzF to FL-T140 was performed in the absence and presence of a 100-fold excess of unlabeled T140. The band on the anti-fluorescein blot disappeared in the presence of excess T140. (f) Crosslinking results for CXCR4 189azF to FL-T140. Crosslink was specific for position 189, but background crosslinking, most likely due to exposure to ambient room light, was detected. Background was not detected when BzF was used as the photocrosslinker.

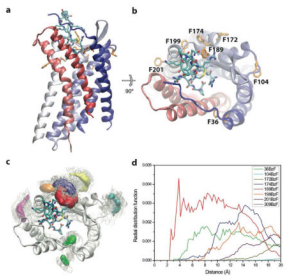

Figure 2.

Molecular modeling of CXCR4 BzF mutants. (a) Crystal structure of CXCR4 bound to CVX15 (cyan) with residues replaced with UAAs highlighted in orange (15). N-terminus of receptor is highlighted in blue and fades to red at the C-terminus. (b) A 90° rotation of the structure in e, which shows a view from the extracellular side of the receptor. (c) Crystal structure of CXCR4 (grey) bound to CVX15 (stick representation). The side-chain modeling determined 100 potential orientations of BzF at each site examined in the crosslinking experiments, and are highlighted on the structure in stick form. The colored density maps indicate the location of the BzF carbonyl for all potential orientations of BzF at each position. Position 309 is not shown because this view is from the extracellular side of the receptor. (d) A graph of the radial distribution function *versus* the distance. Distance measurements were made from the carbonyl in BzF to the closest atom in the CVX15 peptide. The graph for position 309 is not visible on this plot because the distance to the ligand is greater than 20 Å. This graph shows that for position 189, CVX15 has the highest probability of being within the reactive radius of 3.1 Å from the carbonyl group in BzF (21). This supports the data that position 189 is the most likely site to form a crosslink out of the positions examined. From this model, the predicted crosslink site on the ligand is Arg11, which is conserved in both CVX15 and T140. Note this crosslink is independent of the methionine “magnet” effect (24).